

## Magnetostatic interactions in artificial ferrimagnet based magnetic tunnel junctions

C. Tiusan,<sup>a)</sup> T. Dimopoulos, L. Buda, V. Da Costa, and K. Ounadjela

*Institut de Physique et de Chimie des Matériaux de Strasbourg, 23 rue di Loess, F-67037, Strasbourg Cedex, France*

M. Hehn

*Laboratoire de Physique des Matériaux, UMR CNRS 7556, BP 239, 54506 Vandoeuvre lés Nancy, Cedex, France*

H. van den Berg

*Siemens AG, ZT MF1, Paul Gossen Strasse 100, Erlangen D-91052, DE, Germany*

Magnetostatic interactions between the soft and the hard magnetic electrodes in magnetic tunnel junctions (MTJs) using artificial ferrimagnets (AFis) are analyzed. We attribute these interactions to the dispersion fields associated to magnetic inhomogeneities arising from domain walls due to local anisotropic ordering. These magnetostatic interactions can be controlled by adjusting the net magnetic moment of the AFi to optimize the magnetotransport response of the MTJ devices. © 2001 American Institute of Physics. [DOI: 10.1063/1.1360678]

The increasing interest in magnetic tunnel junctions (MTJs) for spin electronic devices requires the understanding and control of the magnetic properties of their ferromagnetic (FM) electrodes. Beyond aspects concerning interfacial magnetism of ferromagnetic/metal insulator interfaces in MTJs, an important parameter is the coupling between the two electrodes of the MTJ. The interactions between the magnetically hard (reference) and the soft (detection) layer of the MTJ are of particular importance as they influence the reversal characteristics of the FM layers and thus the magnetoresistive behavior of the tunnel device.

Several mechanisms can be involved to explain magnetic coupling between two FM films separated by a thin insulating layer: (a) direct FM coupling associated to discontinuity of the insulator, i.e., pinholes; (b) coupling induced by the tunneling of spin polarized electrons<sup>1</sup> such as interfacial effective exchange or exchange dissipative coupling, depending on the dc bias voltage of the MTJ; and (c) magnetostatic coupling. In this last category, one can classify, first, coupling related to the topography of interfaces,<sup>2,3</sup> second, coupling related to dispersion fields associated to magnetic inhomogeneities in the FM electrodes,<sup>4,5</sup> and third, antiferromagnetic coupling related to the lateral closure of the stray fields between the magnetic layers of the MTJ. This latter type of coupling becomes significant when reducing the lateral size of the MTJ electrodes and increasing their aspect ratio. Assuming a continuity and good quality of the MTJ insulating layer, the coupling mainly originates from magnetic interactions. In comparison with previously reported

results,<sup>4,5</sup> this article provides evidence that a major contribution to the magnetostatic coupling originates from the stray field of the domain walls present in the hard subsystem which act as pinning centers in the detection layer. This study has been performed on continuous films and square shaped MTJs having a lateral size of 10  $\mu\text{m}$  to reduce the dipolar antiferromagnetic coupling with respect to the other magnetostatic couplings. We illustrate explicitly the effect of the magnetostatic coupling on the transport and magnetic properties of these systems.

The tunnel junctions consist of the following stack:<sup>6,7</sup> a highly conductive and extremely smooth buffer layer Cr(1.6 nm)/Fe(6 nm)/Cu(30 nm) is grown on a Si(111) wafer. On top of the buffer, the artificial ferrimagnet (AFi) trilayer CoFe(1.8 nm)/Ru(0.8 nm)/CoFe(3 nm) is deposited. The AFi is separated by a 1–2 nm thick Al oxide barrier from a CoFe(1 nm)/Fe(6 nm) magnetically soft subsystem or detection layer (DL). Finally, the multilayer stack is protected with Cu(5 nm)/Cr(3 nm).

Several mechanisms related to magnetostatic interactions are identified between the different components of the junctions as illustrated in Figs. 1(a), 1(b), and 1(c). Reversal features of the MTJ DL [Fig. 1(a)] reveal domain wall blocking phenomena and bias offset measured in the minor tunnel magnetoresistance (TMR) curves. Indeed, the detection layer exhibits a sharp reversal from the antiparallel (high resistive state  $R_{\text{AP}}$ ) to the parallel state (low resistive state  $R_{\text{P}}$ ) which are defined by the direction of the net magnetic moment of the AFi and the magnetization of the detection layer. This sharp reversal is accomplished within a field of about 40 Oe. In contrast, the DL reversal in the opposite direction consists of several successive steps, revealing domain wall blocking phenomena. In this case a field of 70 Oe is required for the

<sup>a)</sup>Author to whom correspondence should be addressed; electronic mail: tiusan@ipcm.u-strasbg.fr

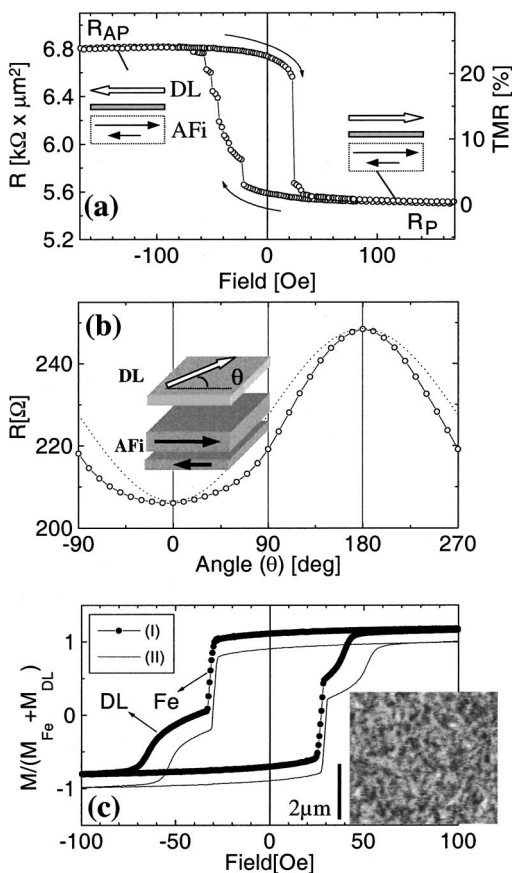


FIG. 1. (a) Minor resistance field curve measured on a CoFe/Ru/CoFe/ $\text{AlO}_x$ /CoFe/Fe MTJ. Arrows illustrate magnetizations in the AFi layers (black) and in the DL (white); (b) (—O—) resistance vs rotating field,  $\theta$  being the angle between the magnetizations in the DL and the AFi and theoretical cosine expectation for this variation (—). (Inset) Sketch indicating the orientation of magnetization in the AFi (black arrows) and DL (white arrow); (c) Minor magnetization curve for continuous film MTJ stack measured in two distinct configurations: (—●—) the AFi has a nonzero net moment (remanent state), and (—) the AFi is demagnetized (zero net moment). (Inset) MFM image of the AFi remanent state, measured with a scan lift of 30 nm similar to the Cu thickness. Therefore, the measured stray fields are similar to those probed by the Fe of the buffer layer.

completion of the reversal process. Additional evidence of existing couplings between the layers is shown in [Fig. 1(b)]. The angular measurement is performed in a limited rotating field of 80 Oe in order to preserve the AFi magnetization rigid and to control only the angular position of the DL with respect to the AFi. The angular dependence of the resistance deviates from the theoretical expected *cosine* function.<sup>1</sup> The ferromagnetic coupling manifests by a broadening of the  $R(\theta)$  curve around the parallel configuration ( $\theta=0$ ) and in a narrowing around the antiparallel configuration ( $\theta=\pi$ ). This set of measurements has been performed for bias voltage applied to the junction ranging from 5 to 100 mV. No variation of the coupling with dc bias was detected. Moreover, the intensity of the coupling was found to increase when decreasing the barrier thickness and when increasing the net magnetic moments of the DL and AFi layers. Therefore, the FM coupling present in this system is purely magnetostatic.

Magnetometry experiments using alternating gradient field magnetometer [Fig. 1(c)] performed on continuous films show coupling effects similar to the patterned junctions in a field window  $H = \pm 100$  Oe where the AFi is magnetically rigid. The only contributions shown in [Fig. 1(c)] come from the reversal of the detection layer and the Fe seed layer present in the buffer. For the Fe seed layer and the detection layer, the  $M-H$  curve is shifted by an offset of  $\sim 10$  and  $\sim 20$  Oe, respectively. Demagnetizing the AFi leads to the vanishing of the offset. We note here that for multilayer stacks without AFi (samples with single Fe layer) no biasing effect is measured. Thus we can exclude any possibility of artifacts due to the measurement technique.

Usually, the FM magnetostatic couplings in a MTJ stack are attributed to the “orange peel” coupling<sup>2,3</sup> originating from correlated rough interfaces of the FM electrodes adjacent to the barrier. In the case under study in this article, we have used the Fe seed layer to distinguish between the different contributions of the magnetostatic couplings. Indeed, the magnetization of the detection and the Fe layers reverse in the same field window [Fig. 1(c)]. The Fe seed is separated from the AFi by a 30 nm thick Cu layer, which prevents the existence of either orange peel magnetostatic type of coupling or direct Ruderman–Kittel–Kasuya–Yosida interactions across this thick Cu layer. However, a field offset of  $\sim 10$  Oe can be measured on the curve obtained with the AFi in a remanent configuration. Previous work<sup>7</sup> has shown that the AFi at low field presents local fluctuations of magnetization related to local anisotropic ordering leading to the formation of  $360^\circ$  domain walls. The stray fields associated to these magnetic inhomogeneities influence significantly the local field experienced by a “neighboring” magnetic layer, consequently contributing to a net pinning field.

A model for explaining these interactions is illustrated in Fig. 2. This figure depicts the magnetic moments of the AFi, the DL, and the Fe in the buffer layer. Small angular fluctuations of magnetization inside the AFi polycrystalline layers give rise to local charge accumulations standing for local dipoles. These charge accumulations become stronger in the case of the presence of  $360^\circ$  domain walls that have been shown to exist in this system.<sup>7</sup> When the AFi is in its antiferromagnetic configuration with the net moment aligned along the field direction, the resultant stray field associated to these dipoles can be probed by the detection layer  $H_d^{\text{DL}}$  and also by the Fe “detector”  $H_d^{\text{Fe}}$ , even at 30 nm. The resulting field is oriented along the AFi net moment and it acts as a positive biasing field during the DL and Fe magnetization reversal. So, it is equivalent to a FM coupling. The presence of these dipoles is confirmed by the magnetic force microscopy (MFM) images of the AFi “remanent” state (Fig. 2, DL layer). The black (white) contrasts correspond to repulsive (attractive) interactions of the MFM tip with the stray fields from the local charge accumulations. When the AFi is demagnetized, the magnetization of each grain is randomly oriented (inset Fig. 1). This situation corresponds to a resulting zero stray field.

A micromagnetic calculation estimates the stray field of a  $360^\circ$  wall located in a 3 nm thick Co layer to values of about 75 Oe at 30 nm from the core of the wall while it

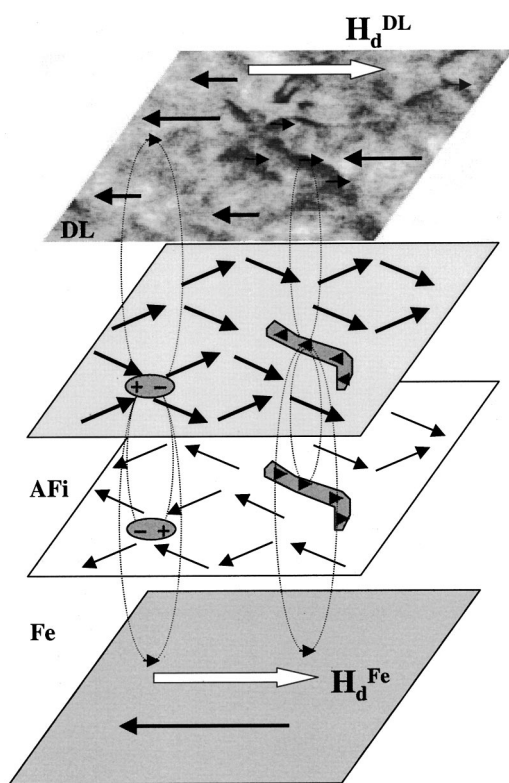


FIG. 2. (Top) Domain structure measured during the reversal of DL for applied field about 20 Oe. The sketch outlines a 2D (top MFM image) and the Fe buffer layer (bottom panel) probe the stray fields emerged from: (i) local anisotropy induced angular fluctuations of magnetization which give rise to local dipoles denoted (+ -) and from (ii)  $360^\circ$  domain wall structures located in the AFi layers (middle panels). Nonzero resulting stray fields bias the DL ( $H_d^{DL}$ ) and the Fe layer  $H_d^{Fe}$ . Their direction is represented by thick large white arrows. Black arrows indicate the local magnetic moment orientation in the DL, AFi, and Fe layers; small white arrows depict the orientation of magnetization in the center of DWs located in the DL and AFi layers. Gray regions in the AFi layers indicate the location of  $360^\circ$  domain walls.

reaches about 500 Oe at 3 nm. When taking into account the granular structure of each magnetic layer, this calculated stray field is reduced by averaging over the volume of the magnetic grains.<sup>5</sup> Moreover, the domain structure in one layer of an AFi is antiferromagnetically duplicated in the other by the strong antiferromagnetic (AF) coupling.<sup>7</sup> From the estimated stray fields, one should subtract the opposite oriented stray field contribution associated to AF mirrored domain wall (DW) structures in the thinner AFi layer. Therefore, the effective fields probed by the DL and the Fe layer are significantly reduced with respect to the theoretical micromagnetic estimation and can be in quantitative agreement

with experimental results measured from the offset in the TMR- $H$  and  $M$ - $H$  curves [Figs. 1(a)–1(c)].

In conclusion, the local stray fields associated to DW located in the AFi layers are responsible to the local pinning of DW in the DL during its reversal. In Fig. 2, we have shown the existence of stable DW configurations in the DL during its reversal measured at a field of about 20 Oe. These domain walls are responsible for the discrete steps present in the negative TMR branch shown in Fig. 1(a), corresponding to the DL reversal from a parallel to an antiparallel magnetization configuration.

The interaction mechanisms between the active magnetic layers of any MTJ device is a key parameter for optimizing their magnetoresistive response. This article gives insight into an important class of magnetostatic interactions associated to dispersion fields emerging from DWs. These effects are related to the randomly distributed anisotropy in polycrystalline films. By inducing a uniaxial anisotropy in the AFi by pinning it with an antiferromagnet the formation of DWs during the reversal process would be inhibited. Therefore, the coupling effects related to DWs or magnetization fluctuations should be drastically diminished.

Another important aspect, with regard to potential applications of MTJs, is the adjustable reduction of these stray fields by using an AFi. Indeed, the stray fields are compensated between the two antiparallel oriented magnetic layers of the AFi. Residual stray fields still subsist because of the nonzero net moment but they are drastically reduced in comparison with a single layer situation.

The authors thank U. Ebels for illuminating discussions and C. Meny, M. Acosta, Y. Henry, and G. Wurz for experimental support. This work was supported by the European Framework IV Materials Technology Program, Contract No. BRPR-CT98-0657, the Dynaspin program, Training and Mobility of Researchers network, under Contract No. FMRX-CT97-0147, and the Nanomem Programme (Grant No. IST-1999-13741). K.O. also acknowledges NSF Grant No. CNRS-9603252.

<sup>1</sup>J. C. Slonczewski, Phys. Rev. B **39**, 6995 (1989).

<sup>2</sup>L. Néel, C. R. Acad. Sci. **255**, 1676 (1962).

<sup>3</sup>S. Demokritov, E. Tsybal, P. Grünberg, W. Zinn, and I. K. Schuller, Phys. Rev. B **49**, 720 (1994).

<sup>4</sup>A. Anguelouch, B. Shrang, G. Xiao, Y. Lu, P. Trouilloud, W. J. Gallagher, and S. S. P. Parkin, Appl. Phys. Lett. **76**, 622 (2000).

<sup>5</sup>L. Thomas, M. G. Samant, and S. S. P. Parkin, Phys. Rev. Lett. **84**, 1816 (2000).

<sup>6</sup>C. Tiusan, M. Hehn, K. Ounadjela, Y. Henry, J. Hommet, C. Meny, H. A. M. van den Berg, L. Baer, and R. Kinder, J. Appl. Phys. **85**, 5276 (1999).

<sup>7</sup>C. Tiusan, T. Dimopoulos, K. Ounadjela, M. Hehn, H. A. M. van den Berg, Y. Henry, and V. Da Costa, Phys. Rev. B **61**, 580 (2000).